example, a mixture of 1.82 g (5.0 mmol) of hydrazide **5a** and 1.14 g (1.25 equiv) of benzaldehyde diethyl acetal was heated at 80 °C, with vigorous stirring, in 50 mL of freshly distilled DMF containing a catalytic amount of TsOH.[13] Solution (bright yellow) was generally obtained within 1 h, and after a total of 5 h the reaction was concentrated and the residue crystallized (*n*-PrOH) to give 1.88 g (83%) of adduct **9a** (Scheme IV, R, R′ = phenyl).[14] Similarly prepared were the following (R′ = phenyl): (compound, R, % yield): **9b**, *p*-methoxyphenyl, 90%; **9c**, *p*-methylphenyl, 91%; **9d**, *p*-nitrophenyl, 52%; **9e**, 2-furyl, 68%; **9f**, 2-thienyl, 80%; **9g**, H, 64%. It is interesting to note that in no case could we detect a measurable quantity of adduct having the α-configuration at C-6.[15]

The extraordinary selectivity of these reactions is easily rationalized on the basis of severe nonbonded interactions in transition state **8b** (cf. Scheme IV). In agreement with this hypothesis, with R′ = H (**5b**),[16] up to 5% of the epimeric material **10** could be observed in the crude reaction mixtures. Of greater importance, however, the stereochemical consequences of kinetic control could be readily reversed upon equilibration. Thus, for example, with R = CO_2Me (R′ = phenyl), our preliminary results indicate that the α configuration is favored to the extent of at least 98:2 at thermodynamic equilibrium.[8a] This latter material, we believe, has all of the functionality requisite for its eventual conversion to **4**, and studies are currently under way with the goal of achieving this transformation.

Acknowledgment. Financial support of this work by the donors of the Petroleum Research Fund (8706-G1), administered by the American Chemical Society, is gratefully acknowledged. The Varian XL-200 spectrometer used in this work was financed in part by the National Science Foundation (CHE-79-08593), the Dreyfus Foundation, and Wesleyan University.

Supplementary Material Available: Fractional coordinates, temperature factors, bond distances, bond angles, crystallographic details, and ORTEP drawing of **9a** (7 pages). Ordering information is given on any current masthead page.

(13) All of these reactions are highly dependent upon the nature of the solvent, proceeding only moderately well in acetonitrile and not at all in glyme or less polar solvents [cf. P. K. Kadaba, *Synthesis*, 71 (1973)]. Furthermore, they fail completely in the absence of TsOH. TsOH, we believe, serves only in the capacity of bringing about an initial ionization of the aldehyde acetal, which is subsequently trapped by the strongly basic nitrogen of hydrazide **5a**. In accordance with this hypothesis, the relative rates for these conversions varied in a manner fully consistent with the ability of R to stabilize a developing cationic center (i.e., **9b**, **9e** > **9a**, **9c**, **9f** > **9g** > **9d**). Aliphatic acetals either fail to react under these conditions or they give much lower yields of adducts (17% with phenylacetaldehyde diethyl acetal).

(14) The stereochemistry of this adduct was conclusively demonstrated by X-ray analysis.[15] Physical properties of adduct **9a**: mp 258–259 °C; IR 1710 cm^{-1}, five-membered ring lactam; NMR ($CDCl_3$) δ 2.02 (2 H, m), 2.82 (1 H, d, J = 17.4 Hz), 2.88 (4 H, m), 2.94 (1 H, d, J = 17.4 Hz), 3.98 (1 H, d, J = 14.1 Hz), 4.33 (1 H, d, J = 5.1 Hz), 4.58 (1 H, s), 4.88 (1 H, d, J = 14.1 Hz), 4.99 (1 H, d, J = 5.1 Hz), 5.90 (1 H, s), 7.23–7.44 (10 H, m).

(15) We are grateful to Drs. James Springer and Karst Hoogsteen, of the Merck Sharp and Dohme Research Laboratories, for carrying out an X-ray analysis on adduct **9a**.

(16) This modest, but reproducible, enhancement is undoubtedly a reflection of decreased steric crowding in transition state **8b**. **5b** was prepared by the reaction of 1-*tert*-butoxycarbonyl-1-methylhydrazine with **15** followed by TFA catalyzed decarboxylation (cf. K. A. Jensen, U. Anthoni, B. Kägi, C. Larsen, and C. T. Pedersen, *Acta Chem. Scand.*, **22**, 1 (1968).

First Manganese(III) Spin Crossover and First d^4 Crossover. Comment on Cytochrome Oxidase

P. Greig Sim and Ekk Sinn*

Department of Chemistry, University of Virginia
Charlottesville, Virginia 22901

Received April 7, 1980

Although the phenomenon of spin-state crossover has been observed in d$^{5-8}$ transition-metal complexes and is theoretically possible in d^4 systems, it has not previously been observed in d^4 systems. Nearly all known manganese(III) complexes are high spin (^{5}E in O_h). The only known low-spin manganese(III) compound is $[Mn(CN)_6]^{3-}$.[1,2] For example, the dithiocarbamate ligands can induce intermediate- and low-spin behavior in iron(III),[3] but manganese(III) is the only case with a theoretical choice of spin states for which all the tris(dithiocarbamate) complexes are high spin.[4] The observation that pyrrole, and especially pyrrole bound up in the ligand TRP [tris[1-(2-azolyl)-2-azabuten-4-yl]amine] (**1**), induces a very strong ligand field[5] prompted us to make a study of [Mn(TRP)]. This choice is justified by the spin-state crossover found to occur in [Mn(TRP)]. The magnetic moment and susceptibility alter dramatically in the 40–50 K region (Figure 1). The moment falls from 4.9 to 3.2 μ_B, corresponding to a change from four to two unpaired electrons. This is a nominally $^5E_g \rightleftarrows {}^3T_{1g}$ spin-state crossover, in O_h symmetry. Above the crossover point the moment is temperature invariant, as expected in ^{5}E, and below 40 K the behavior is compatible with the temperature dependence characteristic of a $^3T_1$ ground state split by spin–orbit coupling and distortion from O_h symmetry.

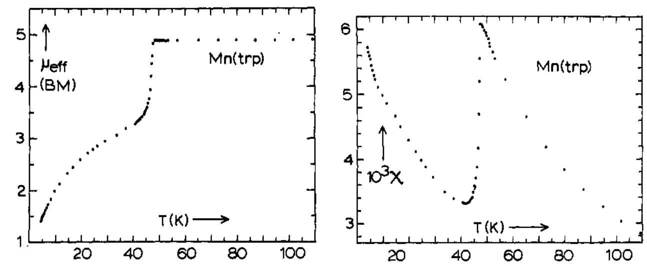

Figure 1. (Left) Magnetic moments and (right) susceptibilities of [Mn(TRP)] at various temperatures.

The crystal structure was determined to shed further light on the manganese environment.[6] Table I gives the resulting atomic parameters, Tables II and III give the bond lengths and angles, and Figure 2 shows the molecular structure. For comparison, bonding data for the related, low-spin [Fe(TRP)] complex are given. The experimental details are as given elsewhere.[5] The metal atom lies on a crystallographic threefold axis so that the three CH_2–CH_2–N–CH–C_4H_4N arms of the ligand are structurally identical. The coordination is distorted about the threefold axis from octahedral toward trigonal-prismatic symmetry, with a twist angle of ϕ = 50.8° defined by projections of the two equilateral NNN ligand triangles (Figure 2). Values of 60° and 0° for ϕ are conditions for octahedral and trigonal-prismatic geometries, respectively. The trigonal distortion splits the $^3T_1$ state in [Mn(TRP)] into a $^3A_1$ and ^{3}E. If the crystal-field splitting is about 25 000 cm^{-1}, the low-temperature magnetic data correspond to a $^3T_1$ splitting of about 150 cm^{-1} and spin–orbit coupling of about −180 cm^{-1}, though these values are not unique.[7]

The observed ϕ value compares with less trigonally distorted [Fe(TRP)] with a twist angle of 54.6°.[5] The difference in twist angles between the iron and manganese complexes is as expected from the shorter metal–ligand bond lengths in the iron complex if the ligand "bite" remains approximately constant. The difference in metal–ligand bond lengths between the two complexes arises from two factors: (1) mainly their different spin states, high spin in manganese(III) (at room temperature) and low spin

(1) Charles, I. D.; Frank, M. J. *J. Inorg. Nucl. Chem.* **1970**, *32*, 555.
(2) Cooke, A. H.; Duffies, H. J. *Proc. Phys. Soc. London, Sect. A* **1955**, *A68*, 32.
(3) Ewald, A. H.; Martin, R. L.; Sinn, E.; White, A. H. *Inorg. Chem.* **1969**, *8*, 1837.
(4) Golding, R. M.; Healy, P.; Newman, P.; Sinn, E.; Tennant, W. C.; White, A. H. *J. Chem. Phys.* **1970**, *52*, 3105.
(5) Sim, P. G.; Sinn, E. *Inorg. Chem.* **1978**, *17*, 1288.
(6) Crystal data [Mn(TRP)]: $MnN_7C_{21}H_{24}$, mol wt 429, space group $I\bar{4}3d$, a = 20.309 (6) Å, V = 8377 Å^3, Z = 16, μ(Mo Kα) = 6.85 cm^{-1}; θ–2θ data collected in the range 1° < 2θ < 48° produced 663 independent reflections, of which 169 were nonsystematically absent; R = 5.9% for 494 reflections.
(7) A detailed treatment of the magnetism will be presented elsewhere.

0002-7863/81/1503-241$01.00/0

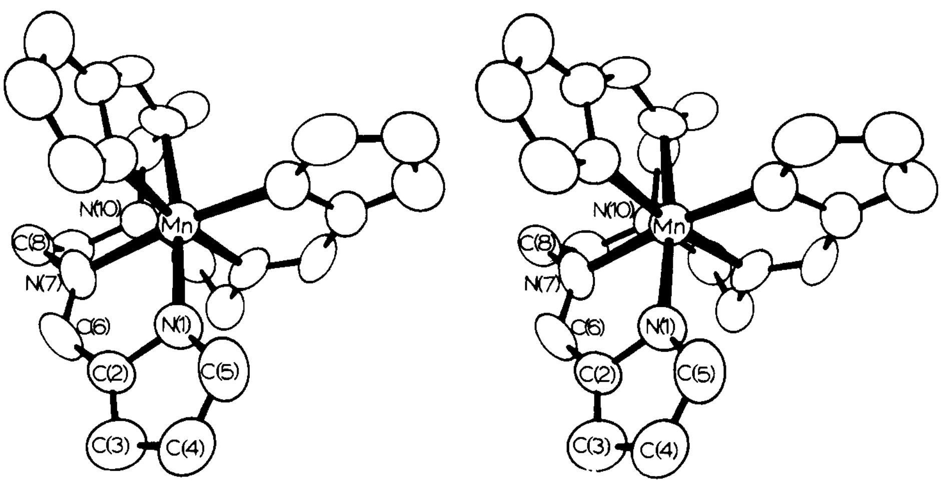

Figure 2. Stereoview of the [Mn(TRP)] molecule.

Table I. Positional and Thermal Parameters and Their Estimated Standard Deviations[a]

atom	x	y	z	B_{11}	B_{22}	B_{33}	B_{12}	B_{13}	B_{23}
Mn	0.1684 (2)	0.1684 (2)	0.1684 (2)	4.0 (1)	4.0 (1)	4.0 (1)	−0.2 (2)	−0.2 (2)	−0.2 (2)
N(1)	0.2692 (3)	0.1615 (3)	0.1660 (4)	4.3 (3)	4.1 (3)	4.6 (3)	−0.1 (3)	−0.4 (3)	−0.7 (3)
N(7)	0.1817 (4)	0.0635 (3)	0.1658 (4)	5.3 (4)	3.5 (3)	3.9 (3)	0.5 (3)	−1.6 (3)	0.5 (3)
N(10)	0.0757 (10)	0.0757 (0)	0.0757 (0)	4.1 (8)	4.1 (8)	4.1 (8)	−0.1 (9)	−0.1 (9)	−0.1 (9)
C(2)	0.2928 (4)	0.0962 (5)	0.1673 (5)	4.5 (4)	4.8 (4)	4.4 (4)	1.0 (4)	0.2 (4)	−0.1 (4)
C(3)	0.3593 (5)	0.0973 (5)	0.1647 (5)	5.3 (5)	7.1 (6)	4.8 (5)	−0.3 (5)	−0.1 (5)	−1.0 (5)
C(4)	0.3790 (5)	0.1607 (5)	0.1634 (5)	5.2 (5)	6.4 (5)	5.3 (5)	−1.5 (5)	−0.6 (4)	−0.2 (5)
C(5)	0.3216 (6)	0.1988 (5)	0.1646 (5)	9.2 (7)	4.1 (4)	4.0 (4)	−0.4 (5)	−0.4 (5)	−1.1 (4)
C(6)	0.2423 (5)	0.0477 (4)	0.1687 (4)	5.9 (4)	3.6 (3)	3.9 (4)	2.1 (4)	−1.5 (4)	−0.7 (4)
C(8)	0.1300 (5)	0.0142 (5)	0.1638 (6)	5.0 (4)	4.1 (4)	5.8 (5)	0.8 (4)	−0.0 (5)	−0.2 (5)
C(9)	0.0992 (4)	0.0124 (5)	0.0978 (5)	4.6 (4)	4.2 (4)	5.6 (5)	−1.3 (4)	0.1 (4)	−1.6 (4)
H(3)	0.400 (5)	0.057 (4)	0.170 (5)	6 (2)					
H(4)	0.417 (4)	0.182 (3)	0.161 (4)	4 (2)					
H(5)	0.317 (4)	0.239 (4)	0.164 (3)	3 (2)					
H(6)	0.250 (3)	0.014 (3)	0.172 (3)	1 (1)					
H(81)	0.153 (4)	−0.025 (4)	0.186 (4)	3 (2)					
H(82)	0.093 (4)	0.033 (3)	0.188 (3)	2 (2)					
H(91)	0.061 (4)	−0.017 (4)	0.103 (4)	5 (2)					
H(92)	0.133 (4)	−0.004 (4)	0.070 (4)	3 (2)					

[a] The form of the anisotropic thermal parameter is $\exp[-(B_{11}h^2a^{*2} + B_{22}k^2b^{*2} + B_{33}l^2c^{*2})/4 + (B_{12}hka^*b^* + B_{13}hla^*c^* + B_{23}klb^*c^*)/2]$.

Table II. Bond Distances and Closest Intermolecular Contact (Å)

	Mn	Fe		Mn	Fe
M-N(1)	2.054 (2)	1.936 (1)	C(2)-C(3)	1.353 (4)	1.389 (8)
M-N(7)	2.148 (2)	1.989 (1)	C(2)-C(6)	1.423 (4)	1.411 (8)
M-N(10)	3.259 (2)	3.304 (1)	C(3)-C(4)	1.658 (5)	1.382 (8)
N(1)-C(2)	1.409 (3)	1.379 (3)	C(4)-C(5)	1.398 (5)	1.387 (8)
N(1)-C(5)	1.306 (4)	1.347 (3)	C(8)-C(9)	1.479 (5)	1.524 (8)
N(7)-C(6)	1.272 (4)	1.288 (4)	Mn-Mn[a]	4.690 (1)	
N(7)-C(8)	1.452 (4)	1.463 (4)			
N(10)-C(9)	1.443 (3)	1.435 (4)	⟨C-H⟩	0.94	

[a] Nearest intermolecular Mn-Mn distance.

in iron(III), and (2) partly the slightly greater size of manganese(III) over iron(III) in the same spin states due to the nuclear charge difference. The average metal–ligand bond length difference, 0.14 Å, is felt more in the metal–amino nitrogen bond (0.16 Å) than in the metal–pyrrole bonds (0.12 Å).

There is additional distortion in each complex which lowers the symmetry further. The twist angle ϕ is determined by the relative positions of two equilateral NNN triangles each perpendicular to the threefold axis, but the triangles are inequivalent. In [Fe(TRP)], the angle subtended at the iron atom by two adjacent pyrrole nitrogen atoms [N(1)–Fe–N(1′)] is 93.22° while for adjacent amino nitrogens [N(7)–Fe–N(7′)] this is 97.89°. For

Table III. Bond Angles (Degrees)

	Mn	Fe		Mn	Fe
N(1)-M-N(7)[a]	78.81 (10)	81.06 (3)	N(1)-C(2)-C(3)	108.8 (2)	109.1 (1)
N(1)-M-N(10)	121.53 (9)	122.95 (3)	N(1)-C(2)-C(6)	114.1 (3)	113.3 (1)
N(7)-M-N(10)	59.12 (9)	60.55 (3)	C(3)-C(2)-C(6)	137.1 (3)	137.6 (1)
N(1)-M-N(1)	95.15 (9)	93.22 (3)	C(2)-C(3)-C(4)	108.2 (3)	107.0 (1)
N(7)-M-N(7)	96.01 (9)	97.89 (3)	C(3)-C(4)-C(5)	106.4 (3)	106.9 (1)
N(1)-M-N(7)[b]	90.52 (9)	87.87 (3)	N(1)-C(5)-C(4)	111.0 (3)	110.2 (1)
N(1)-M-N(7)[c]	172.08 (10)	174.23 (3)	N(7)-C(8)-C(9)	110.4 (3)	110.9 (1)
M-N(1)-C(2)	113.69 (18)	114.27 (4)	N(10)-C(9)-C(8)	113.6 (2)	113.5 (1)
M-N(1)-C(5)	140.7 (2)	138.85 (4)			
C(2)-N(1)-C(5)	105.6 (2)	107.87 (8)			
C(9)-N(10)-C(9)	118.0 (2)	119.48 (8)			
M-N(7)-C(6)	111.8 (2)	113.9 (1)			
M-N(7)-C(8)	126.4 (2)	125.2 (1)			
C(6)-N(7)-C(8)	121.8 (2)	120.9 (1)			

[a] Within the same ligand arm. [b] Adjacent ligand arms. [c] N(1), N(7) opposite.

[Mn(TRP)] these angles do not differ as dramatically, having values of 95.15 and 96.01°, respectively, but the difference between the Mn–N bonds (0.094 Å) is greater than that in the iron complex (0.053 Å). In each complex the triangle formed from the pyrrole nitrogens [N(1)] is smaller than that from the imine nitrogen atoms [N(7)]. The sides of these triangles have lengths of 3.03 and 3.19 Å in [Mn(TRP)] and 2.81 and 3.00 Å in [Fe(TRP)].

Magnetically coupled d^5–d^9 complexes have been of considerable interest as cytochrome *c* oxidase models[8–13] because of the enzyme's anomalous magnetic properties, which could be rationalized in terms of a strong Fe–Cu coupling, $J \sim -300$ cm^{-1}. However, no proven models for such a system yet exist. Synthetic coupled d^5–d^9 complexes, of which we have made the first and the most strongly coupled,[12] have only shown coupling constants about an order of magnitude too small. On treatment with CN^- the resting oxidase exhibits a temperature-dependent magnetic moment which can be interpreted in terms of a coupled low-spin d^5–d^9 system, with $J \sim -40$ cm^{-1}.[9] A d^4 high-spin–low-spin equilibrium in a d^4–d^{10} [Fe(IV)–Cu(I)] system with the metals well separated would adequately explain the magnetic properties, and a d^4–d^{10} model is otherwise at least as plausible, based on recent work with the enzyme.[13] Such an explanation has not come readily to mind in the past in the absence of evidence for d^4 spin crossovers. With the clear observation of a spin equilibrium in d^4, both models must now seriously be considered and compared.

Acknowledgment. Support received under NSF Grant CHE77-01372 is gratefully acknowledged.

Supplementary Material Available: A listing of F_o and F_c (3 pages). Ordering information is given on any current masthead page.

(8) Van Gelder, B. F.; Beinert, H. *Biochim. Biophys. Acta* **1975**, *400*, 439. Griffith, J. S. *Mol. Phys.* **1971**, *21*, 141.
(9) Tweedle, M. F.; Wilson, L. J.; Garcia-Iniguez, L.; Babcock, G. T.; Palmer, G. *J. Biol. Chem.* **1978**, *253*, 8065.
(10) Reed, C. A.; Landrum, J. T. *FEBS Lett.* **1979**, *106*, 265.
(11) Petty, R. H.; Welch, B. R.; Wilson, L. J.; Bottomley, L. A.; Kadish, K. M. *J. Am. Chem. Soc.* **1980**, *102*, 611.
(12) Gruber, S. J.; Harris, C. M.; Sinn, E. *J. Chem. Phys.* **1968**, *49*, 2183. Kokot, S.; Harris, C. M.; Sinn, E. *Austr. J. Chem.* **1972**, *25*, 45. Freyberg, D. P.; O'Connor, C. J.; Sinn, E. *Inorg. Chem.* **1979**, *18*, 1077.
(13) Seiter, C. H. A.; Angelos, S. G. *Proc. Natl. Acad. Sci. U.S.A.* **1980**, *77*, 1806.

A New Aqueous Chemistry of Organometallic, Trinuclear Cluster Compounds of Molybdenum

Avi Bino*

Department of Inorganic and Analytical Chemistry
The Hebrew University of Jerusalem
Jerusalem, Israel

F. Albert Cotton

Department of Chemistry, Texas A&M University
College Station, Texas 77843

Zvi Dori

Department of Chemistry, Israel Institute of Technology
Haifa, Israel

Received September 24, 1980

The reactions of $Mo(CO)_6$ and $W(CO)_6$ with acetic acid are important, interesting and, especially for $Mo(CO)_6$, complicated. We have previously reported[1,2] that for $W(CO)_6$ products can be isolated that contain either the trinuclear cluster species $[W_3(\mu_3\text{-}O)_2(OAc)_6(H_2O)_3]^{2+}$ or a substitution product thereof with H_2O replaced by, e.g., OAc^-. The reaction of $Mo(CO)_6$ yields

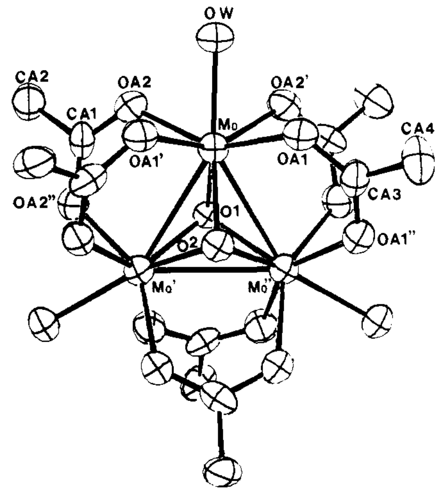

Figure 1. $[Mo_3O_2(OAc)_6(H_2O)_3]^{2+}$ ion found in compounds **1** and **2**.

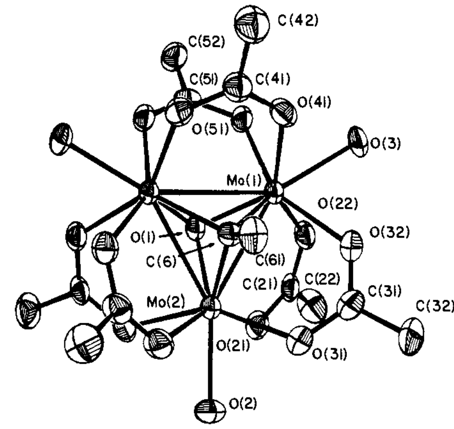

Figure 2. $[Mo_3O(CCH_3)(OAc)_6(H_2O)_3]^+$ ion found in compound **3**.

$Mo_2(OAc)_4$ (ca. 15%) and a solution from which several trinuclear products can be isolated, either directly or following reaction with an oxidizing agent. One of these was previously reported[3] and assigned the formula $[Mo_3(OEt)_2(OAc)_6(H_2O)_3](CF_3SO_3)_2$. A thorough reinvestigation of this system has led to the recognition of a remarkable class of new compounds and shows that the above formula should be revised.

We describe six representative compounds that illustrate the nature and range of the field. All are obtained from the reaction of $Mo(CO)_6$ with a refluxing mixture of AcOH and $(AcO)_2O$, followed by suitable workup,[4] and have been identified by

(1) Bino, A.; Cotton, F. A.; Dori, Z.; Koch, S.; Küppers, H.; Millar, M.; Sekutowski, J. C. *Inorg. Chem.* **1978**, *17*, 3245.
(2) Bino, A.; Hesse, K.-F.; Küppers, H. *Acta Crystallogr., Sect. B* **1980**, *B36*, 723.
(3) Bino, A.; Ardon, M.; Maor, I.; Kaftory, M.; Dori, Z. *J. Am. Chem. Soc.* **1976**, *98*, 7093.

(4) The ions of compounds **4** and **5** were obtained as previously described.[3] Elution of the cation-exchange column with $NaSbF_6$, CF_3SO_3H, or $CH_3C_6H_4SO_3H$ followed by slow evaporation afforded **4**, **5**, or 6, respectively, in crystalline form. Compounds **1** and **2** are best obtained by refluxing $Mo(CO)_6$ in an AcOH/$(AcO)_2O$ mixture for 24 h with constant bubbling of air. After being cooled, the solution was filtered, diluted with water, and passed through a Dowex 50W-X2 cation-exchange column. Elution of the adsorbed red ion with 0.5 M HBr or CF_3SO_3H followed by slow evaporation led to compounds **1** and **2**. When the $M(CO)_6$ reaction is carried out in the presence of NaOAc, an orange solid was obtained upon evaporation of the mother liquor. This solid was dissolved in water and the solution treated as described above. Elution of the orange ion with 0.1 M HBF_4 followed by slow evaporation led to the isolation of compound **3**. In all cases small amounts of $Mo_2(OAc)_4$ precipitated from the reaction mixture and were separated by filtration.

(5) Satisfactory elemental analyses have been obtained for all new compounds. To illustrate how analytical data support CH_3C caps, are less compatible with CH_3CH_2O caps, and rule out CH_3O caps, we give carbon analyses (%) for **5** and **6**. The percentages found are averages of several, highly reproducible analyses. Anal. (for compound **5**) Calcd: CH_3C, 20.63; CH_3CH_2O, 19.94; CH_3O, 18.19. Found: 20.62 ± 0.06. (for compound **6**) Calcd: CH_3C, 28.46; CH_3CH_2O, 27.66; CH_3O, 26.38. Found: 28.66 ± 0.06. In the case of **1** the oxidation number of molybdenum was shown by permanganate titration, similar to that used for the tungsten compounds,[1] to be +4.0 ± 0.1.

